

THE NATURE OF THE BRIGHT SUBMILLIMETER GALAXY POPULATION:
A RADIO-PRESELECTED SAMPLE WITH $I > \sim 25$

S. C. CHAPMAN,¹ E. A. RICHARDS,^{2,3} G. F. LEWIS,⁴ G. WILSON,^{5,6} AND A. J. BARGER^{3,5,7,8}

Received 2000 October 25; accepted 2000 November 27; published 2001 February 19

ABSTRACT

Deep submillimeter surveys have successfully detected distant, star-forming galaxies, which are enshrouded in vast quantities of dust and emit most of their energy at far-infrared wavelengths. These luminous galaxies are an important constituent of the universal star formation history, and any complete model of galaxy evolution must account for their existence. Although these sources have been tentatively identified with very faint and sometimes very red optical counterparts, their poorly constrained redshift distribution has made their interpretation unclear. In particular, it was not understood if these galaxies had been missed in previous surveys or if they constituted a truly new class of objects, undetectable at other wavelengths. By utilizing a radio selection technique, we have isolated a sample of 20 submillimeter objects representative of the 850 μm population brighter than 5 mJy with $z \leq 3$. We show that these galaxies are so heavily dust-obscured that they remain essentially “invisible” to ultraviolet selection. Furthermore, relying on the radio/submillimeter flux density ratio, we estimate their redshift distribution, finding a median of two. These results are inconsistent with the existence of a very high redshift ($z > 4$) population of primeval galaxies ($L_{\text{bol}} > 10^{12} L_{\odot}$) contributing substantially to the submillimeter counts. While not a substitute for the thorough follow-up of blank-field submillimeter surveys, our results do shed light on a substantial portion of the luminous submillimeter population with $z \leq 3$.

Subject headings: galaxies: clusters: general — galaxies: evolution — galaxies: formation —
radio continuum: galaxies — submillimeter

On-line material: color figures

1. INTRODUCTION

The extragalactic far-infrared background light is believed to be composed of the integrated thermal starlight and nonthermal active galactic nucleus (AGN) radiation, reradiated by dust within star-forming galaxies over the entire history of galaxy formation. The energy density of this infrared background is approximately the same as that found in the optical, suggesting that at least half of the universal star formation history remains hidden from optical view (Puget et al. 1996). This diffuse background was first resolved into discrete sources by the Submillimeter Common-User Bolometer Array (SCUBA; Holland et al. 1999) on the James Clerk Maxwell Telescope (JCMT) by a number of groups (Smail, Ivison, & Blain 1997; Hughes et al. 1998; Barger et al. 1998; Eales et al. 1999).

Although a large number of deep SCUBA surveys have led to a better estimate of the 850 μm galaxy surface density, our understanding of the nature of the submillimeter population remains limited. The principal obstacle is obtaining reliable counterparts of these submillimeter sources at other wavelengths, a problem exacerbated by both the coarseness of the JCMT resolution (15" at 850 μm) and the inherent faintness of suspected optical counterparts (Smail et al. 1999). It is still unclear whether the submillimeter-selected sources are related

to known populations, such as high-redshift quasars (Hughes, Dunlop, & Rawlings 1997; McMahon et al. 1999) or Lyman break galaxies (LBGs; Chapman et al. 2000), or constitute a truly new class of objects. With the exception of several isolated objects, few reliable identifications have been made (e.g., Ivison et al. 1998; Frayer et al. 1998). Thus, the redshift distribution has remained largely unconstrained over a vast range, with the possibility that many sources lie at extreme distances ($z > 5$).

One technique, which has shown some promise in identifying submillimeter sources, is radio continuum follow-up. Because galaxies and the intergalactic medium are transparent at centimeter wavelengths, radio emission is unhindered by intervening gas and dust. Ubiquitous in local star-forming galaxies, radio emission also correlates very strongly with the far-infrared emission in star-forming galaxies (Helou, Soifer, & Rowan-Robinson 1986). Moreover, the high resolution provided by radio interferometers can provide a surrogate for the poor submillimeter angular resolution and astrometric uncertainties.

Given the difficulties of obtaining secure optical identifications and spectroscopic redshifts, the radio observations provide another clue to the nature of submillimeter sources. Via the empirically observed far-infrared to radio correlation in local star-forming galaxies, one can use the observed ratio of submillimeter to radio continuum flux density to estimate a redshift. As the k -corrections (corrections based on the redshifted spectral energy distribution [SED]) of the radio and submillimeter flux densities are opposite in slope, the ratio of radio to submillimeter flux density is quite sensitive to redshift (Carilli & Yun 1999).

Barger, Cowie, & Richards (2000, hereafter BCR) first attempted to use a radio-selected sample to target a number of optically faint microjansky radio sources with near-infrared magnitude, $K > 20.5$. Using SCUBA to a 3 σ rms limiting flux density of 6 mJy at 850 μm , they detected five out of 15 radio sources, while in the process demonstrating that none of the

¹ Observatories of the Carnegie Institution of Washington, 813 Santa Barbara Street, Pasadena, CA 91101.

² Department of Physics, University of Alabama, Huntsville, AL 35899.

³ Hubble Fellow.

⁴ Anglo-Australian Observatory, P.O. Box 296, Epping, NSW 1710, Australia.

⁵ Institute for Astronomy, University of Hawaii, 2680 Woodlawn Drive, Honolulu, HI 96822.

⁶ Physics Department, Brown University, Providence, RI 02912.

⁷ Department of Astronomy, University of Wisconsin, 475 North Charter Street, Madison, WI 53706.

⁸ *Chandra* Fellow at Large.

TABLE 1
RADIO AND SUBMILLIMETER PROPERTIES OF OUR
NEW SCUBA OBSERVED SOURCES

Source	$S_{1.4\text{ GHz}}$ (μJy)	$S_{850\text{ }\mu\text{m}}$ (mJy)	z_{CY}^a	$z_{450/850}^b$
Detected				
VLA J123521+620720	143 \pm 13.2	8.3 \pm 2.8	2.2 $^{+1.2}_{-0.8}$	N.A.
VLA J123551+620809	98.7 \pm 10.3	5.5 \pm 1.8	2.0 $^{+1.1}_{-0.8}$	>1.7
VLA J123553+621337	58.4 \pm 9.00	8.8 \pm 2.1	2.9 $^{+1.4}_{-1.0}$	>1.1
VLA J123555+620901	212 \pm 13.7	5.4 \pm 1.9	1.3 $^{+0.9}_{-0.6}$	>1.0
VLA J123600+620253	262 \pm 17.1	6.9 \pm 2.0	1.5 $^{+0.9}_{-0.6}$	>1.9
VLA J123606+621021	74.4 \pm 9.00	11.6 \pm 3.5	3.0 $^{+1.5}_{-1.0}$	N.A.
VLA J123624+621743	78.8 \pm 9.10	10.4 \pm 3.4	2.9 $^{+1.4}_{-1.0}$	N.A.
VLA J123649+615930	264 \pm 18.4	3.5 \pm 1.2	1.0 $^{+0.8}_{-0.5}$	>0.5
VLA J123650+622732	660 \pm 35.8	4.7 \pm 1.6	0.6 $^{+0.4}_{-0.3}$	>0.5
VLA J123708+622201	170 \pm 12.8	10.2 \pm 2.7	2.0 $^{+1.2}_{-0.8}$	>1.3
VLA J123710+622650	551 \pm 30.6	7.4 \pm 2.2	1.0 $^{+0.8}_{-0.5}$	>0.4
VLA J123711+621331	132 \pm 10.1	7.7 \pm 2.4	2.0 $^{+1.2}_{-0.8}$	N.A.
VLA J123713+621826	595 \pm 30.9	15.7 \pm 2.4	1.4 $^{+0.9}_{-0.6}$	>0.9
Undetected				
VLA J123521+615926	378 \pm 25.9	-0.6 \pm 2.5	<1.0	...
VLA J123522+620953	117 \pm 11.9	0.7 \pm 2.1	<1.6	...
VLA J123527+621937	193 \pm 14.7	-1.2 \pm 2.1	<1.2	...
VLA J123547+621529	118 \pm 10.6	2.3 \pm 1.6	<1.4	...
VLA J123551+622514	354 \pm 22.2	2.0 \pm 1.9	<0.9	...
VLA J123604+620811	55.4 \pm 9.10	2.1 \pm 2.4	<2.2	...
VLA J123604+621620	80.6 \pm 9.30	2.1 \pm 2.2	<1.9	...
VLA J123611+622149	111 \pm 11.4	-0.9 \pm 2.2	<1.6	...
VLA J123622+620654	159 \pm 11.7	3.2 \pm 2.3	<1.4	...
VLA J123643+622511	202 \pm 15.4	1.5 \pm 2.2	<1.2	...
VLA J123649+620738	307 \pm 17.4	-0.7 \pm 2.2	<1.0	...
VLA J123659+621832	506 \pm 30.2	-4.6 \pm 3.0	<0.9	...
VLA J123709+622258	708 \pm 36.9	3.2 \pm 1.9	<0.6	...
VLA J123718+620355	6580 \pm 330	-0.5 \pm 3.7	<0.02	...

NOTE.— SEDs similar to Arp 220 are assumed for the redshift estimates. All sources have $I > 25$, the 5σ completeness limit of our optical imagery. Radio source coordinates can be found in Richards (2000).

^a Redshift estimates from the submillimeter/radio index using the Carilli & Yun (2000) indicator.

^b An independent check on the submillimeter/radio redshift estimates through the 450/850 μm limit (e.g., Hughes et al. 1998) and a dust temperature $T_d = 45$ K, consistent with Arp 220. The 450 μm measurement is often not sufficient to provide a useful limit (listed “N.A.”).

optically brighter radio sources ($K < 20.5$) were detected in the submillimeter. The surface density of these few bright radio-selected submillimeter sources closely matched that from blank-field surveys, indicating a close correspondence between the optically faint radio population and bright submillimeter sources. Other pointed SCUBA studies of known high- z populations such as $z \sim 3$ LBGs (Chapman et al. 2000) and radio-loud AGNs (Archibald et al. 2001) have revealed few SCUBA detections and nowhere near the surface density of blank-field submillimeter sources.

We have refined the selection criterion to those microjansky radio sources with an optical magnitude, $I > 25$, based on the clear bimodal break in the optical properties of microjansky radio sources (Richards et al. 1999). We have applied this technique to a sample in the region surveyed by Richards (2000) centered on the Hubble Deep Field (HDF). We have selected a total of 47 radio sources in our study, 20 previously observed, that meet our criterion. Our follow-up SCUBA photometry observations of 27 radio-selected objects demonstrate this to be a highly successful technique. We now detect $\sim 50\%$ of the new 27 object sample above 4.5 mJy at 850 μm , with an overall success rate of 20 out of 47 objects observed. Our increased

detection success over BCR is likely to be a result of our slightly deeper survey coupled with the stricter selection criterion. We are thus able to uncover bright submillimeter sources using SCUBA at the rate of one source per hour on the JCMT, greater than an order of magnitude more rapid than mapping a random patch of sky. Our new survey represents a submillimeter mapping of a ~ 100 arcmin² effective region in less than 16 hr, sensitive to sources $S_{850} > 5$ mJy and $z \lesssim 3$.

2. SOURCE SELECTION AND SUBMILLIMETER OBSERVATIONS

The HDF region has previously been imaged at 1.4 GHz using the Very Large Array (VLA) radio telescope by Richards (2000) to a completeness of 40 μJy . We aligned a deep I -band optical image described in Barger et al. (1999a, 1999b) with the VLA FK5 astrometric frame by using 102 of 333 radio sources that lie within the 30' \times 30' optical field of view. After alignment, 60 radio sources were determined not to have any optical identifications within 2" of the radio position brighter than $I < 25$. Of these, 17 have previously been described in Richards et al. (1999). Several of these were followed up as part of the submillimeter study of BCR. Of the increased sample of 60 optically faint radio objects, we chose to concentrate on the 40 that had previously not been observed by BCR or Hughes et al. (1998). Time constraints allowed us to observe only 27 of these, although these were selected at random with no further selection bias.

We observed each of the radio sources using the JCMT/SCUBA at 850/450 μm in photometry mode for an effective integration time between 600 and 2000 s. The secondary was chopped at 7.8125 Hz, using a chop throw ($\sim 50''$) and direction chosen to keep the source in a bolometer throughout the observation. Pointing was checked before and after the observation on blazars, and sky dipo were performed to measure the atmospheric opacity directly. The rms pointing errors were below 2", while the average atmospheric zenith opacities at 450 and 850 μm were 1.7 and 0.24, respectively. The data were reduced using the Starlink package SURF (SCUBA User Reduction Facility; Jenness, Lightfoot, & Holland 1998), and our own reduction routines were used to implement the three-bolometer chopping mode. Spikes were first carefully rejected from the data, followed by correction for atmospheric opacity and sky subtraction using the median of all the array pixels, except for obviously bad pixels and the source pixels. The data were then calibrated against standard planetary and compact H II region sources observed during the same nights. Our 13 new source detections above 3σ at the positions of $\sim 10\sigma$ radio detections are stronger than isolated 3σ measurements on their own.

In addition, we reanalyzed the SCUBA data from BCR and found their source 3 to have a 3σ detection (5.3 ± 1.7 mJy), which we include in our present sample. We also include the submillimeter source HDF 850.2 from the Hughes et al. (1998) study, having a radio source counterpart $S_{1.4} > 40$ μJy and $I > 25$ (Richards 1999).

3. ANALYSIS AND DISCUSSION

The crucial data available to us from our technique are the optical properties and redshift estimates for the submillimeter sources, which we present in Table 1. Our results assume a $\Lambda = 0.0$, $\Omega = 1.0$, $H_0 = 65$ km s⁻¹ Mpc⁻¹ cosmology. Redshift estimates can be obtained from the submillimeter/radio flux ratios (Carilli & Yun 2000). All of our submillimeter sources fall roughly in the redshift range $z = 1-3$ with a median redshift

for the sample of $z = 1.9$, consistent with previous results from BCR. The sensitivity of our radio survey to star-forming galaxies with radio luminosities fainter than 10^{24} W Hz $^{-1}$ diminishes quickly past $z \sim 3$ and hence biases our submillimeter survey. An independent check on the submillimeter/radio redshift estimates can be obtained through the 450/850 μm ratio (e.g., Hughes et al. 1998). Subject to unknown dust temperature, we obtain an estimate of $T_d/(1+z)$, which we list in Table 1 for $T_d = 45$ K for consistency with the ultraluminous infrared galaxy, Arp 220. Raising or lowering the adopted dust temperature has the effect of a corresponding systematic raising and lowering of both our redshift estimates (Blain 1999).

The area covered by the radio is exactly the sensitivity-weighted primary beam discussed in Richards (2000), where the nonuniform sensitivity effects were dealt with in order to calculate the proper radio source counts. The question is over how large an area one can detect a radio source of given flux density without an $I < 25$ optical counterpart. The way to calculate this is to take each of the radio sources in the survey, determine the radio visibility area, then compare this number to the area the optical image covers (about $25' \times 25'$ to account for the stars and bad parts of the CCDs), and sum. The central region of the VLA image has one such source per 0.3 arcmin 2 .

Our preselected sample has already saturated the bright (>5 mJy) submillimeter counts (Fig. 1), and there are not likely to be many additional bright, high-redshift submillimeter sources in our survey region. Given the effects of large-scale structure on the source counts, the best comparison is with blank-field surveys of the same region. This is possible for subsets of our survey area, where BCR found that two additional submillimeter sources without radio counterparts were detected, indicating 75% of the bright submillimeter sources are typically recovered through such radio preselection. Borys et al. (2000) uncovered a similar fraction of bright submillimeter sources without radio counterparts in a ~ 100 arcmin 2 SCUBA scan map of the extended HDF. Since we performed photometry on the sources, we have no means of estimating this extra population over the full survey area. By accounting for such an additional 25% high-redshift population, our sample is in agreement with analyses of the redshifts for lensed submillimeter sources (Barger et al. 1999a, 1999b; Smail et al. 2000; Blain et al. 1999a). The percentage of submillimeter sources missed by our preselection technique will depend field to field on the high- z clustering of submillimeter luminous sources. A lensed submillimeter survey (Smail et al. 2000) detects a similarly large fraction of their bright submillimeter sources in the radio. Deeper blank-field submillimeter surveys (e.g., Eales et al. 2000; $S_{850 \mu\text{m}} \geq 3$ mJy) detect about one-third of their sources in the radio. This is roughly in agreement with our results, which use deeper radio maps and brighter submillimeter limits. While not a substitute for the thorough (and difficult) follow-up of blank-field submillimeter surveys, our results do shed light on a substantial portion of the luminous submillimeter population with $z \leq 3$.

Although we are sensitive only to sources with $S_{850} \geq 5$ mJy, we can deduce important properties about the fainter submillimeter population. Averaging our submillimeter undetected sample (inverse variance weighted) reveals a mean flux of $S_{850} = 0.8 \pm 0.3$ mJy, suggesting that many of these, $\sim 50\%$ of our $I > \sim 25$ and $S_{1.4} > 40$ μJy radio sample, are still fairly luminous submillimeter sources. They likely form a continuous distribution with the $S_{850} \geq 5$ mJy sample, lie at similar or lower redshifts (Table 1), and comprise roughly 10% of the blank-field SCUBA source counts from 1 to 5 mJy. This leaves a

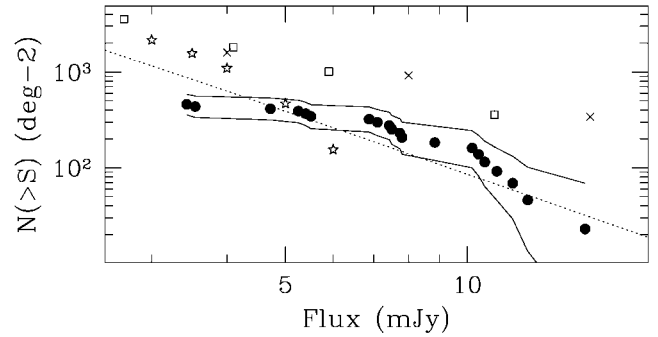


FIG. 1.—Integrated source counts estimated from our optically faint radio source sample (filled circles). The jagged solid lines are 1σ uncertainties. Also plotted are the fit to blank-field submillimeter survey counts from BCR (dotted line), the counts of Eales et al. (2000; stars), and the lensing amplified counts of Blain et al. (1999b; crosses) and Chapman et al. (2001; squares). Our radio-selected sources saturate the bright submillimeter counts, and there are not likely to be many additional bright, high-redshift submillimeter sources in our survey region. [See the electronic edition of the Journal for a color version of this figure.]

large portion of submillimeter sources fainter than 5 mJy that are not subsumed in our present $I > 25$, $S_{1.4} > 40$ μJy radio sample.

One possibility is that many of these fainter submillimeter sources are contained in our present radio surveys but are actually optically bright ($I < 25$). While no LBGs have been found with $S_{850} > 5$ mJy, a few red and bright LBGs are known to emit at $S_{850} \geq 2$ mJy (Chapman et al. 2001a, 2000), with a statistical detection of high star formation rate LBGs at ~ 0.7 mJy (Chapman et al. 2001a). These must contribute some fraction of the missing sources. This is consistent with the high star formation rate deduced by Steidel et al. 1999, who apply a large dust correction to their results. Our Arp 220 SED model suggests that these sources would be detected in our present radio survey beyond $z = 2$. However, the HDF-SCUBA results (Hughes et al. 1998; Peacock et al. 2000) also show directly that a significant fraction of the ~ 2 mJy sources are not associated with bright LBGs. Although deeper radio observations with optically faint counterparts may quickly recover this population, it also remains a possibility that these sources represent high-redshift ($z > 4$) protogalaxies with $L_{\text{bol}} < 10^{12} L_{\odot}$, which would remain undetected in the radio to significantly deeper flux limits. So by pushing to fainter radio limits, it is rather unclear what types of objects might be preselected.

An additional concern with the submillimeter source population is that massive AGNs may be heating the dust rather than star formation. We can be reasonably certain that our radio-selected submillimeter sources are not driven primarily by AGNs for two reasons. First, the sources are spatially resolved with a median of about $2''$ in the radio using the Merlin interferometer at a resolution of $0''.2$ (Richards 2000; Muxlow et al. 2000), corresponding to ~ 1 kpc at $z = 2$ for our adopted cosmology. If the radio and associated submillimeter emission were emanating from such a compact active nucleus (an AGN), it would appear unresolved even at this fine resolution. Second, the submillimeter sources have recently been shown to have little or no overlap with X-ray sources as observed with the *Chandra* satellite (e.g., Fabian et al. 2001; Hornschemeier et al. 2000; Barger et al. 2001). As scenarios that would obscure even the X-ray emission are improbable, the implication is that most bright submillimeter sources are in fact driven by star formation.

Assuming then that our radio-selected sources are driven primarily by star formation, it is appropriate to use our data to estimate a contribution to the comoving star formation rate density (SFRD). In Figure 2, we integrate over our measured counts in three redshift bins, and divide by the effective volume of our detected sources, to represent the submillimeter SFRD as a function of redshift. Since we have assumed the far-IR/radio relation in the redshift estimates, our SFRD estimates can be derived from either wavelength in a manner similar to BCR. We plot our new points as filled squares (submillimeter-detected objects) and a filled hexagon (submillimeter-undetected objects). The very high redshift open square ($z > 3$) represents the Hubble Flanking Fields submillimeter sources undetected in the radio from BCR and Borys et al. 2000. We then compare optically selected sources (*open triangles*) at redshifts $1 < z < 4$ (Connolly et al. 1997; Steidel et al. 1999). We apply a dust correction to the optical points for $z > 1$, using the Steidel et al. (1999) prescription (factor of ~ 5 for $z > 2$). This is roughly in accord with the expected correction from the Chapman et al. (2001a) submillimeter measurement of 33 LBGs with large expected star formation rates. Lower redshift radio-selected sources with bright optical counterparts, as analyzed by Haarsma et al. (2000), are also plotted (*open circles*), requiring no correction factor for dust obscuration.

Submillimeter sources fainter than 5 mJy likely begin to merge with optically selected samples (e.g., Adelberger & Steidel 2000). However, our $I > 25$ radio-selected population is truly an orthogonal population to those discovered in optical surveys, even for $S_{850} \lesssim 5$ mJy. We can then confidently sum the optically selected (but uncorrected for dust; $I < 25$) and submillimeter ($I > 25$) points from $z = 1-4$ to arrive at a conservative lower limit to the total SFRD of all presently known objects (*large stars with arrows*). This lower limit can be compared with the dust-corrected optical points, which is still a rather uncertain procedure.

We have therefore recovered the majority of the bright (> 5 mJy) submillimeter sources with a statistically significant sample, selected based on the microjansky radio emission with extremely faint optical counterparts. We can state with some assurance that the bulk of bright submillimeter-selected sources represent a highly dust-obscured star-forming population that would be very difficult to identify in optically based surveys. Our redshift analysis has also demonstrated that this is not because the submillimeter sources are at very high redshifts ($z \gg 3$). These sources may represent the epoch in which the most massive spheroid galaxies were being formed through merging fragments in cluster environments. Indeed, the recent identification of prodigious submillimeter emission with highly overdense cluster cores at $z \sim 3$ and $z \sim 3.8$ (Chapman et al. 2001c and Ivison et al. 2000, respectively) suggests that the most luminous members of our submillimeter source sample may highlight similar such regions. Pushing our study to fainter submillimeter and radio flux limits will facilitate our understanding of the transition and overlap between these ultra-luminous high- z star formers (which may evolve into the most

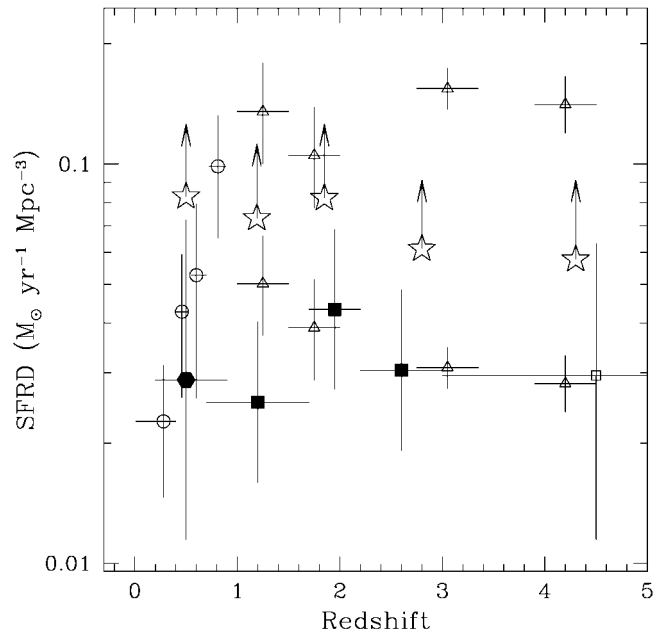


FIG. 2.—SFRD as a function of redshift. Measurements are obtained by integrating over the source counts and dividing by the effective volume of the detected sources (assuming a $\Lambda = 0$, $\Omega = 1$, $H_0 = 65 \text{ km s}^{-1} \text{ Mpc}^{-1}$ cosmology). Our new submillimeter points are represented as filled squares (submillimeter-detected sources) and a filled hexagon (submillimeter-undetected sources), while the very high redshift point ($z > 3$; *open square*) represents the submillimeter sources undetected in the radio from BCR. Compare these points with optically selected samples with and without dust corrections (see text) over the range $1 < z < 4$, represented as open triangles (Connolly et al. 1997; Steidel et al. 1999) and radio-selected samples (Haarsma et al. 2000) with confirmed optical counterparts ($I < 25$), plotted as open circles. The optical and submillimeter measured points thus plotted represent essentially orthogonal galaxy populations ($I > 25$ and $I < 25$), and we can confidently sum the optically selected (but uncorrected for dust; $I < 25$) and submillimeter ($I > 25$) points from $z = 1$ to 4 to arrive at a conservative lower limit to the total SFRD of all presently known objects (*large stars with arrows*). This lower limit can be compared with the dust-corrected optical points, still a rather uncertain procedure. [See the electronic edition of the Journal for a color version of this figure.]

massive spheroids in the present epoch) and the less massive galaxies selected in the optical through the Lyman break technique (Steidel et al. 1999).

We thank the staff of the JCMT for their assistance with the SCUBA observations. The James Clerk Maxwell Telescope is operated by the Joint Astronomy Centre on behalf of the Particle Physics and Astronomy Research Council of the UK, the Netherlands Organization for Scientific Research, and the National Research Council of Canada. E. A. R. and A. J. B. acknowledge support by NASA through Hubble Fellowship grants HF-01123.01A and HF-01117.01A awarded by the Space Telescope Science Institute, which is operated by the Association of Universities for Research in Astronomy, Inc., for NASA under contract NAS5-26555.

REFERENCES

- Adelberger, K. L., & Steidel, C. C. 2000, *ApJ*, 544, 218
 Archibald, E., et al. 2001, *MNRAS*, in press
 Barger, A. J., Cowie, L. L., & Richards, E. A. 2000, *AJ*, 119, 2092 (BCR)
 Barger, A. J., Cowie, L. L., Sanders, D. B., Fulton, E., Taniguchi, Y., Sato, Y., Kawara, K., & Okuda, H. 1998, *Nature*, 394, 248
 Barger, A. J., Cowie, L. L., Smail, I., Ivison, R. J., Blain, A. W., & Kneib, J.-P. 1999a, *AJ*, 117, 2656
 Barger, A. J., Cowie, L. L., Trentham, N., Fulton, E., Hu, E. M., Songaila, A., & Hall, D. 1999b, *AJ*, 117, 102
 Barger, A. J., Cowie, L., Mushotzky, R., & Richards, E. 2001, *AJ*, in press (astro-ph/0007175)
 Blain, A. W. 1999, *MNRAS*, 309, 955
 Blain, A. W., Jameson, A., Smail, I., Longair, M. S., Kneib, J.-P., & Ivison, R. J. 1999a, *MNRAS*, 309, 715
 Blain, A. W., Kneib, J.-P., Ivison, R. J., & Smail, I. 1999b, *ApJ*, 512, L87
 Borys, C., Chapman, S. C., Halpern, M., & Scott, D. 2000, in *Deep Submillimeter Surveys* (astro-ph/0009143)
 Carilli, C., & Yun, M. 1999, *ApJ*, 513, L13

- . 2000, *ApJ*, 530, 618
- Chapman, S. C., Scott, D., Borys, C., & Halpern, M. 2001a, in *Deep Submillimeter Surveys* (astro-ph/0009152)
- Chapman, S. C., Scott, D., Borys, C., & Fahlman, G. 2001b, *MNRAS*, in press (astro-ph/0009134)
- Chapman, S. C., et al. 2000, *MNRAS*, 319, 318
- Chapman, S. C., Lewis, G. F., Scott, D., Richards, E., Borys, C., Steidel, C. C., Adelberger, K. L., & Shapley, A. E. 2001c, *ApJ*, 548, L17
- Connolly, A., et al. 1997, *ApJ*, 486, L11
- Eales, S., et al. 1999, *ApJ*, 515, 518
- . 2000, *AJ*, 120, 2244
- Fabian, A., et al. 2001, *MNRAS*, 321, L33
- Frayer, D., et al. 1998, *ApJ*, 506, L7
- Haarsma, D. B., Partridge, R. B., Windhorst, R. A., & Richards, E. A. 2000, *ApJ*, 544, 641
- Helou, G., Soifer, B. T., & Rowan-Robinson, M. 1986, *ApJ*, 298, L7
- Holland, W., et al. 1999, *MNRAS*, 303, 659
- Hornschemeier, A. E., et al. 2000, *ApJ*, 541, 49
- Hughes, D. H., Dunlop, J. S., & Rawlings, S. 1997, *MNRAS*, 289, 766
- Hughes, D. H., et al. 1998, *Nature*, 394, 241
- Iverson, R. J., Smail, I., Le Borgne, J.-F., Blain, A. W., Kneib, J.-P., Bézecourt, J., Kerr, T. H., & Davies, J. K. 1998, *MNRAS*, 298, 583
- Iverson, R. J., et al. 2000, *ApJ*, 542, 27
- Jenness, T., Lightfoot, J. F., & Holland, W. S. 1998, *Proc. SPIE*, 3357, 548
- McMahon, R. G., Priddey, R. S., Omont, A., Snellen, I., & Withington, S. 1999, *MNRAS*, 309, L1
- Muxlow, T. W. B., Wilkinson, P. N., Richards, A. M. S., Kellerman, K. I., Richards, E. A., & Garrett, M. A. 2000, *NewA Rev.*, 43, 623
- Peacock, J., et al. 2000, *MNRAS*, 318, 535
- Puget, J.-L., Abergel, A., Bernard, J.-P., Boulanger, F., Burton, W. B., Desert, F.-X., & Hartmann, D. 1996, *A&A*, 308, L5
- Richards, E. A. 1999, *ApJ*, 513, L9
- . 2000, *ApJ*, 533, 611
- Richards, E. A., Fomalont, E. B., Kellermann, K. I., Windhorst, R. A., Partridge, R. B., Cowie, L. L., & Barger, A. J. 1999, *ApJ*, 526, L73
- Smail, I., Iverson, R. J., & Blain, A. W. 1997, *ApJ*, 490, L5
- Smail, I., Iverson, R. J., Kneib, J.-P., Cowie, L. L., Blain, A. W., Barger, A. J., Owen, F. N., & Morrison, G. 1999, *MNRAS*, 308, 1061
- Smail, I., Iverson, R. J., Owen, F. N., Blain, A. W., & Kneib, J.-P. 2000, *ApJ*, 528, 612
- Steidel, C. C., Adelberger, K. L., Giavalisco, M., Dickinson, M., & Pettini, M. 1999, *ApJ*, 519, 1